# 8

## Referências bibliográficas


1. CHAMMAS, Roger. Biologia do câncer: uma breve introdução. “In:” **Tratado de oncologia**. 1.ed. São Paulo: Atheneu, 2012. p.3-7.

2. ALONSO, Daniel; BAL DE KIER JOFFÉ, Elisa; PURICELLI, Lydia. **Biología tumoral, claves celulares y moleculares del cáncer**. 1. ed. Buenos Aires: Eudeba, 2008.

3. LOPES, Aline A.; OLIVEIRA, Andreza M.; PRADO, Camila B. C. Principais genes que participam da formação de tumores. **Revista de biologia e ciências da terra**. v. II, n.II. 2002.

4. Disponível em: < http://www.cancer.gov/about-cancer/what-is-cancer>. Acesso em: 15 junho, 2015.

5. Disponível em: <http://www2.inca.gov.br/wps/wcm/connect/cancer/site/oquee. acesso em: 15 junho, 2015.

6. Disponível em: < http://www.inca.gov.br/enfermagem/docs/cap2.pdf>. Acesso em: 15 junho, 2015.

7. RIVIORI, Augusto W. et. al. Biologia molecular do câncer cervical. **Rev. Bras. Saúde Matern. Infant.**, v. 6, n. 4, p.447-451, out. - dez., 2006.

8. Disponível em: <http://paniaguabio.blogspot.com.br/2013/08/carcinogenese-teoria-dos-multipos.html>. Acesso em: 17 junho, 2015.

9. BORGES-OSÓRIO, M. R.; ROBINSON, W. M. Genética humana. 2. ed. Porto Alegre: Artmed, 2001.

10. GOMES-CARNEIRO, M. R.; RIBEIRO-PINTO, L. F.; PAUMGARTTEN, F. J. R. Fatores de risco ambientais para o câncer gástrico: a visão do toxicologista. **Cad. Saúde Públ.**, v.13(Supl. 1), p.27-38, 1997.

11. JEGGO, Penny A.; PEARL, Laurence H.; CARR, Antony M. DNA repair, genome stability and cancer: a historical perspective. **Nat Rev. Cancer**. v. 16, p. 35-42, jan., 2016.

12. Disponível em : < http://www.inca.gov.br/enfermagem/docs/cap2.pdf>. Acesso em: 02 agosto, 2015.

13. Disponível em : <http://paniaguabio.blogspot.com.br/2013/08/carcinogenese-teoria-dos-multipos.html>. Acesso em: 02 agosto, 2015.

14. MENDELSOHN, John. et al. **The Molecular Basis of Cancer**, 4 ed. Elsevier/Saunders, 2014.

15. HANAHAN, D.; WEINBERG, R. A. Hallmarks of cancer: the next generation. **Cell**, n.144, p.646-674, 2011.

16. GONZÁLEZ, D. J. S.; BAHENA, N. I. T. **Biología celular y molecular**, 1 ed. Alfil,2006.

17. Disponívelem:<http://www.sobiologia.com.br/conteudos/Citologia2/nucleo11.php>. Acesso em; 03 agosto, 2015

18. GUYTON, A. C. H., J. E. A célula e seu funcionamento. "In:" **Guyton & Hall**. **Tratado de Fisiologia**, Elsevier (Ed.). 2006. p.1176.

19. ADAMS, J.M.;CORY, S. The Bcl-2 apoptotic switch in cancer development and therapy. **Oncogene**, v.26, n. 9, p.1324–1337, 2007.

20. LOWE, S.W.;CEPERO, E.; EVAN, G. Intrinsic tumour suppression. **Nature**, n. 432, p.307–315, 2004.

21. CHIN, C.; HARLEY, C. B. Replicative senescence and cell immortality: the role of telomeres and telomerase. **Proc. Soc. Exp. Biol. Med**., p. 99-106, 1997.

22. RUIZ, A.S.; ANGOSTO, M.C. Implicaciones fisiopatológicas de la telomerasa. **Na R Acad Nac Med (Madr)**. v. 117, n. 2, p.427- 444, 2000.

23. YASHIMA, K. et al. Expression of the RNA component of telomerase during human development and differentiation. **Cell Growth Differ**., v.9, n. 9, p.805-813, 1998.

24. O'REILLY, M.S. et al. Angiostatin: a novel angiogenesis inhibitor that mediates the suppressionof metastasis by a Lewis lung carcinoma. **Cell**, v. 79, p. 315-328, 1994.

25. JUNQUEIRA, M. S.; MELO, Fabiana H. M. de ; CHAMMAS, Roger . Mecanismos de invasão e metástases. "In:" Francisco Ricardo Gualda Coelho; et al. **Bases da oncologia**. 2ed. São Paulo: LEMAR, 2003, v. 1, p. 1-452.

26. Disponível em : <http://www.inca.gov.br– fatores de risco Acessado em: 18 de agosto de 2015.

27. Disponível em : http://www.nacc.org.br/infantil/infantil_quimioterapia.shtml>. Acessada em 27 de setembro de 2015.

28. Disponível em: <http://www.iarc.fr/>. Acessada em 27 de setembro de 2015.

29. Disponível em: <http://www.cccancer.net/o-que-e-quimioterapia/>. Acessada em 27 de setembro de 2015.

30. ALMEIDA, V.L.; LEITÃO, A.; REINA, L.C.B.; MONTANARI, C.A.; DONNICI, C.L. Câncer e agentes antineoplásicos ciclo-celular específicos e ciclo-celular não específicos que interagem com o DNA: Uma introdução.**Quim. Nova**, v.28, n.1, p. 118-129, 2005.

31. MURPHY M.; LEVINE, AJ. Tumorsuppressor genes. “In:” Mendelsohn J, et al(eds). **The molecular Basis of cancer**, 2ªed. Philadelphia: WS Saunders, 2001, p. 95- 114.

32. RAJSKI, S. R.; WILLIAMS, R. M.; **Chem Rev**.,v.*98*, p.2723,1998.

33. REMERS, W. A. Antineoplastic agents. “In:” DELGADO, J. N.; REMERS, W. A. **Wilson and Gisvold’s textbook of organic medicinal and pharmaceutical chemistry**. 10th ed. Philadelphia: Lippincott Willians & Wilkins, 1998, cap. 12, p. 343.

34. HAHN, W. C.; WEINBERG, R. A.; **Nat. Rev. Cancer** ; v.*2*, p.331, 2002.

35. SCHARER, O. D.; DNA interstrand crosslinks: natural and drug-induced DNA adducts that induce unique cellular responses; **Chembiochem**, v.6, p.27–32, 2005.

36. NOLL, D. M.; MASON, T. M.; MILLER, P. S.; Formation and repair of interstrand cross-links in DNA. **Chem Rev**., v.106, p.277–301, 2006.

37. GOODMAN, L.; WINTROBE, M.; DAMESHEK, W.; GOODMAN, M.; GILMAN, A.; Nitrogen mustard therapy—use of methyl-bis(beta-chloroethyl)aminehydrochloride and tris(beta-chloroethyl)aminehydrochloride for Hodgkin’s disease, lymphosarcoma, leukemia and certain allied and miscellaneous disorders. **J Am Med Assoc**, v. 132, p.126–132, 1946.

38. GILMAN, A.; PHILIPS, F.; The biological actions and therapeutic applications of the B-chloroethyl amines and sulfides. **Science**, v. 103, p. 409–436, 1946.

39. GEIDUSCHEK, E. P.; ‘‘Reversible’’ DNA.; **Proc Natl Acad Sci USA** , v.47, p.950–955, 1961.

40. KOHN, K. W.; SPEARS, C. L.; DOTY, P.; Inter-strand crosslinking of DNA by nitrogen mustard, **J Mol Biol** , v. 19, p. 266–288, 1966.

41. GUAINAZZI, A.; SCHARER, O. D.; Using synthetic DNA interstrand crosslinks to elucidate repair pathways and identify new therapeutic targets for cancer chemotherapy; **Cell. Mol. Life Sci**..,v. 67, p.3683–3697, 2010.

42. MURAD, A.M.; KATZ, A.; **Oncologia Bases Clínicas do Tratamento**, Guanabara Koogan, Rio de Janeiro, 1996, p. 41.

43. MACHADO, A. E. D. **Quim. Nova**. v.23, p. 237, 2000.

44. OLIVEIRA, R. B.; ALVES, R. J. **Quim. Nova**, v.*25*, p. 976, 2002.

45. OSENBERG, B.; VANCAMP, L.; TROSKO, J. E.; MANSOUR, V. H.; Platinum compounds: a new class of potent antitumour agents, **Nature** , v. 222, p. 385–386, 1969.

46. ROSENBERG, B.; VANCAMP, L, KRIGAS, T.; Inhibition of cell division in Escherichia coli by electrolysis products from a platinum electrode, **Nature**, v. 205, p. 698–699, 1965.

47. JAMIESON, E. R.; LIPPARD, S.; Structure, Recognition, and Processing of Cisplatin-DNA Adducts; **Chem. Rev**., v. 99, p.2467-2498, 1999.

48. HUANG, Z.; et al. Determination of cisplatin and its hydrolytic metabolite in human serum by capillary electrophoresis techniques. **Journal of chromatography A**. n.1106, p. 75-79, 2006.

49. CARADONNA, J.P.; LIPPARD, S.J.; GAIT, M.J.; SINGH, M. The antitumor drug cis-dichlorodiammineplatinum forms an intrastrand d(GpG) crosslink upon reaction with [d(ApGpGpCpCpT)]2. **J. Am. Chem. Soc**., v.104, p.5793–5795, 1982.

50. FONTES, A.P.S.; ELOI, T.C.; BERALDO, H. A Química Inorgânica na Terapia do Câncer. **Cadernos Temáticos de Química Nova na Escola**, n.6, p. 13-18, 2005.

51. WANG, D.*;* LIPPARD, S.J.; Cellular processing of platinum anticancer drugs; **Nature reviews/ Drug Discovery** , v. 4, 2005.

52. PIZARRO, A. M.; SADLER, P. J.; Unusual DNA binding modes for metal anticancer complexes, **Biochimie** , v. 91, p. 1198–1211, 2009.

53. PEREZ,R.S. Cellular and molecular determinants of cisplatin resistance. **Eur. J. Cancer**, v.34, p.1535-1542, 1998.

54. OLIVEIRA, M.C.B.; *et al*. Nucleic acid cleavage by a Cu(II) polyaza macrocyclic complex, **Polyhedron**, v. 24, p. 495–499, 2005.

55. REY, N.A.; et al. A synthetic dinuclear copper(II) hydrolase and its potential as antitumoral: Cytotoxicity, cellular uptake, and DNA cleavage. **Journal of Inorganic Biochemistry**, v. 103, p. 1323-1330, 2009.

56. BALES, B. C.; PITIE, M.; MEUNIER, B.; GREENBERG, M. M.; A Minor Groove Binding Copper-Phenanthroline Conjugate Produces Direct Strand Breaks via $\beta$-Elimination of 2-Deoxyribonolactone, **J. Am. Chem. Soc**., v.124, p. 9062-9063, 2002.

57. HEGG, E. L.; BURSTYN, J.N.; **Coord. Chem. Rev**., v. 173, p. 133–165, 1998.

58. LIU, C.; WANG, M.; ZHANG, T.; SUN, H.; DNA hydrolysis promoted by di- and multi-nuclear metal complexes, **Coord. Chem. Rev**., v. 248, p. 147–168, 2004.

59. KRA¨MER, R.; Bioinorganic models for the catalytic cooperation of metal ions and functional groups in nuclease and peptidase enzymes, **Coord. Chem. Rev**., v.182, p. 243–261, 1999.

60. HECHT, S. M. **Bioinorganic Chemistry: Nucleic Acids.** New York: Oxford University Press, 1996.

61. MITIC, N.; et al; The Catalytic Mechanisms of Binuclear Metallohydrolases, **Chem. Rev**., v. 106, p. 3338-3363, 2006.

62. GOTTLIED, H.E.; KOTLYAR, V.; NUDELMAN, A.; NMR Chemical Shifts of Common Laboratory Solvents as Trace Impurities. **Journal of Organic Chemistry**, v.62, p. 7512-7515, 1997.

63. MOSMANN T. Rapid colorimetric assay for cellular growth and survival: application to proliferation and cytotoxicity assays. **J Immunol Methods**. v.65, p. 55-63, 1983.

64. SCUDIERO, D. A., SHOEMAKER, R. H., PAULL, K. D., MONKS, A., BOYD, M. R. Evaluation of a Soluble Tetrazolium Formazan Assay for Cell Growth and Drug Sensitivity in Culture Using Human and Other Tumor Cell Lines. **Cancer Research**, n.48, v.17, p. 4827-4833, 1988.

65. C. N. VERANI. **Rational Synthesis and Characterization of Paramagnetic Heteropolynuclear Systems Containing [MA-MB-MC], [MA-MB]2 and [M1-2( R)1-2-3] Cores**. Dissertation (Doktor der Naturwissenschaft) - Fakultat fur Chemie, Ruhr-Universitat Bochum, Mulheim an der Ruhr , 2000.

66. NEVES, A.; ERTHAL, S. M. D.; DRAGO, V.; GRIESAR, K. and HAASE, W. A new N,O-donor binucleating ligand and its first iron(III) complex as a model for the purple acid phosphatase. **Inorganica Chimica Acta**, v. 197, p. 121-124, 1992.

67. REY, N. A. **Novos Ligantes Binucleantes e seus Complexos Metálicos do tipo $Cu^{II}$-(Mu-OH)-$Cu^{II}$:** 1) Modelos Estruturais para o Sítio Ativo das Catecol Oxidases e 2) Análogos Sintéticos com Atividade Redox e/ou Hidrolítica. Tese de doutorado, Universidade Federal de Santa Catarina, 2008.

68. BELLAMY, L.J. **The Infrared Spectra of Complex Molecules.** Third ed., Wiley, New York, 1975.

69. SILVERSTEIN, R.M.; et al. **Identificação Espectrofotométrica de Compostos Orgânicos**. 7 ed, LTC, Rio de Janeiro, 2010.

70. KAISER, C. R. RMN 2D: Detecção inversa e gradiente de campo na determinação estrutural de compostos orgânicos. **Qúimica Nova**, v. 23, n. 2, p. 231-236, 2000.

71. SALLES, M. R. Química de Coordenação: fundamentos e atualidades. "In:" **Espectroscopia Eletrônica dos Compostos de Coordenação**, ÁTOMO (Ed.). 2009. p.424.

72. TAMBOURA, F.B.; et al. Dinuclear lanthanide (III) complexes with large-bite Schiffbasesderived from 2,6-diformyl-4 chlorophenoland hydrazides: Synthesis, structuralcharacterization and spec tros opic studies. **Polyhedron**. v. 43, p. 97-103, 2012.

73. EL-SHERIF, A. A. **Inorganica Chimica Acta**. v. 362, p. 4991-5000, 2009.

74. X.H. B; et al. **Inorg. Chim. Acta**. v.308, p.143–149, 2000.

75. NAKAMOTO, K. **Infrared and Raman Spectra of Inorganic and Coordination Compounds.Part B**. Jonh Wiley & Sons, New York, 1997.

76. RODRÍGUEZ-PÁEZ, J. E; et al. Controlled precipitation methods: formation mechanism of ZnO nanoparticles. **Journal of the European Ceramic Society**, v.21, n. 7, p. 925-930, 2001.

77. RODRÍGUEZ-PÁEZ, J. E.; **Estudio de los mecanismos de formación de partículas de ZnO con diseño morfológico y dimensional obtenidas por el método de precipitación controlada**. PhD tesis edition, Universidad Autónoma de Madrid, 1999.

78. BRADLEY, D. C.; MEHROTRA, R. C.; GAUR, D. P.; Metal alkoxides and diketonates. Academic Press,1978.

79. SARIC, A.; POPOVIC, S.; TROJKO, R.; MUSIC, A.; The thermal behavior of amorphous rhodium hydrous oxide. **Journal of Alloys and Compounds**, v.4320, n. 1, p. 140-148, 2001.

80. MORAES, R. S. **Síntese e caracterização de ligantes binucleantes derivados do tuberculostático isoniazida e seus complexos binucleares de cobre(II) com pontes exógenas acetato ou hidroxo**. Dissertação de Mestrado, Pontifícia Universidade Católica do Rio de Janeiro, 2011.

81. ATKINS, A. J. et al. Synthesis and structure of mononuclear and binuclear zinc(ii) compartmental macrocyclic complexes. **Dalton Transactions**, n. 9, p. 1730-1737, 2003.

82. DEACON, G.B.;PHILLIPS, R.J. Ralationships between the carbon-oxygen stretching frequencies of carboxylato complexes and the type of carboxylate coordination. **Coordination Chemistry Reviews,** v.33, p.227-250, 1980.

83. JONES, C. J. **A Química dos Elementos dos Blocos d e f**. Bookman, Porto Alegre, 2002.

84. J.D.LEE. **Quimica inorganica não tão concisa.** 5. ed. São Paulo: Blucher, 1999.

85. HUHEEY,J.E. **Inorganic Chemistry: Principles of Structure and Reactivity**, Harper Collins, New York 1993.

86. NOGUEIRA, Aline Cruz de Moraes Reis. **Contribuição ao estudo da Química de Coordenação dos ligantes compartimentais e suas potencialidades como inibidores de fusão para o tratamento de infecções por HIV**. Tese de Doutorado, Pontifícia Universidade Católica do Rio de Janeiro, 2014.

87. LANZNASTER, Maurício. **Desenvolvimento de novos modelos estruturais e funcionais para as fosfatases ácidas púrpuras**. Tese de Doutorado, Universidade Federal de Santa Catarina, 2003.

88. REIS, Aline Cruz de Moraes et al. Different coordination patterns for two related unsymmetrical compartmental ligands: crystal structures and IR analysis of $[Cu(C_{21}H_{21}O_2N_3)(OH_2)(ClO_4)]ClO_4 \cdot 2H_2O$ and $[Zn_2(C_{22}H_{21}O_3N_2)(C_{22}H_{20}O_3N_2)]ClO_4$. **Journal Of Coordination Chemistry**, v. 67, n. 18, p.3067-3083, 17 set. 2014.

89. LEWIS, D. L.; ESTES, E. D.; HODGSON, D. J.. The infrared spectra of coordinated perchlorates. **Journal Of Crystal And Molecular Structure**. v.5, p. 67-74, 1975.

90. KREBS, B.; SCHEPERS, K.; HENKEL, G.; HENKEL, G.; ALTHAUS, E.; MULLERWARMUTH, W.; GRIESAR, K. and HAASE, W. Model compounds for the oxidized Uteroferrin-phosphate complex with novel dinucleating ligands containing phenolate and pyridine donors. **Inorganic Chemistry**, v. 33, n. 9, p.1907-1914, 1994.

91. GABER, B. P.; MISKOWSKI, V. and SPIRO, T. G. Ressonance ramanscaterring from iro(III)- and copper(II)- transferrin and an iron (III) model compound. A spectroscopic interpretation of transferrin binding

site. J**ournal of American Chemical Society**. v. 96, n. 22, p. 6868-6873, 1974.

92. LIEBER, M.; et al. A continuous tumor-cell line from a human lung carcinoma 102 with properties of type II alveolar epithelial cells. **Int J Cancer**, v. 17, p. 62-70, 1976.

93. KAIHHN, M. E.; et al. Establishment and characterization of a human prostatic carcinoma cell line (PC3). **Invest. Urol**. v.17, p. 16–23, 1979.

94. REY, N.A.; et al.*;* Catalytic Promiscuity in Biomimetic Systems: Catecholase-like Activity, Phosphatase-like Activity, and Hydrolytic DNA Cleavage Promoted by a New Dicopper(II) Hydroxo-Bridged Complex, **Inorganic Chemistry**, v. 46, n. 2, 2007.

95. ZENKOVA, M. A.; **Artificial Nucleases**. 1ª ed. Springer Verlagy NY, USA, 2012.

96. REY, N.A.; et al. A synthetic dinuclear copper(II) hydrolase and its potential as antitumoral: Cytotoxicity, cellular uptake, and DNA cleavage. **Journal of Inorganic Biochemistry**, v. 103, p. 1323-1330, 2009.

97. ROSSI, L.M.; et al; Synthesis, structure and properties of unsymmetrical l-alkoxo-dicopper(II) complexes: biological relevance to phosphodiester and DNA cleavage and cytotoxic activity, **Inorganica Chimica Acta**, v.358, p. 1807–1822, 2005.

# 9

# Anexo

Optical Materials 52 (2016) 188–191

Contents lists available at ScienceDirect

Optical Materials

journal homepage: www.elsevier.com/locate/optmat

## Luminescent properties of a di-hydrazone derived from the antituberculosis agent isoniazid: Potentiality as an emitting layer constituent for OLED fabrication

Rafaela S. Moraes [a], Rian E. Aderne [b], Marco Cremona [b], Nicolás A. Rey [a,*]

[a] Laboratório de Síntese Orgânica e Química de Coordenação Aplicada a Sistemas Biológicos (LABSO-BIO), Departamento de Química, PUC-Rio, Rua Marquês de São Vicente, 225, 22453-900 Gávea, RJ, Brazil
[b] Laboratório de Optoeletrônica Molecular (LOEM), Departamento de Física, PUC-Rio, Rua Marquês de São Vicente, 225, 22453-900 Gávea, RJ, Brazil

ARTICLE INFO

*Article history:*
Received 21 September 2015
Received in revised form 22 December 2015
Accepted 24 December 2015

*Keywords:*
Isonicotinoyl hydrazone
Isoniazid
Luminescence
Emitting layer
OLEDs

ABSTRACT

Hydrazones constitute a class of compounds presenting azomethine R′R″N–N=*CH*–R hydrogens, which show diverse properties and a wide range of applications. A hydrazone derived from the antituberculosis drug isoniazid, namely, *N,N′*-diisonicotinoyl-2-hydroxy-5-methylisophthalaldehyde hydrazone (DMD) was synthesized and chemically characterized. Its luminescent properties were also investigated, as well as the possibility of using this compound as a constituent of the emitting layer for the fabrication of OLEDs. Co-deposited devices were fabricated using the organic molecule BSBF as matrix and DMD as dopant. All the devices presented a broad electroluminescence band, in which it was possible to recognize the DMD emission along with emissions of some of the other organic layers. The best results were obtained with 35% DMD doping, achieving a luminance of about 35 cd/m$^2$.



### 1. Introduction

Hydrazones constitute a class of compounds presenting azomethine R′R″N–N=*CH*–R hydrogens, which have been the subject of investigations due to their diverse properties and a wide range of applications [1]. Such versatility can be attributed to their easy synthesis, modularity and unique structural features, such as (i) both nucleophilic imine and amino-type (more reactive) nitrogen atoms, (ii) an azomethine carbon that has both electrophilic and nucleophilic characters, (iii) a configurational isomerism due to the C=N double bond, and, in most cases, (iv) an acidic N–*H* proton [2]. Several hydrazones are biologically active compounds tested as anticancer [3], antibacterial and antimicrobial agents [4]. This class of compounds has a strong coordinating ability toward different metals [5]; particularly, their transition-metal and lanthanide ions complexes have been used as new materials for the development of potential chemo-sensors [2] as well as for optoelectronic applications [6]. In this context, a variety of charge-transporting materials, such as stilbenes, pyrazolines, arylalkanes, arylamines, carbazoles, or thiophene-containing compounds have been generated; however, hydrazones have advantages over other charge-transporting materials, including a fast transporting ability, high photosensitivity, simple synthesis and low cost [7,8].

The LABSO-BIO research group at PUC-Rio has experience in the synthesis and characterization of hydrazones derived from the antituberculosis agent isonicotinoyl hydrazide (isoniazid) [9,10], with a main focus on their intrinsic biological properties. Recently, for example, it has been proven that one of these compounds, namely, INHHQ, displays potential anti-Alzheimer activity [11]. In addition, the past few years witnessed an approximation endeavor involving the LABSO-BIO and the PUC-Rio Molecular Optoelectronics Laboratory (LOEM) groups, aiming to further develop the potentiality of hydrazones for OLED (organic light emitting diode) fabrication. Mostly due to their applications in different areas and their simplicity of manufacturing, OLEDs allow for the use of different materials to develop novel optoelectronic and photonic devices [12–15]. OLEDs exhibit certain working advantages, such as employing low operating voltages and the possibility of a wide selection of emission colors through the molecular design of their organic constituents. Generally, these electroluminescent (EL) systems are assembled through a heterojunction architecture between three or more organic molecular materials: an electron injection layer, the emitting layer and, finally, the hole injection layer. Research in new electroluminescent materials has led to a continuing quest for novel compounds or their combinations, making it possible to create new applications or improved properties.

* Corresponding author.
*E-mail address:* nicoarey@puc-rio.br (N.A. Rey).

http://dx.doi.org/10.1016/j.optmat.2015.12.039
0925-3467/

In this context, and due to their larger electron delocalization possibilities, we began the studies by using symmetrical isonicotinoyl di-hydrazones, such as the one derived from 2-hydroxy-5-methyl-isophthalaldehyde (Fig. 1, hereafter called DMD). To the extent of our knowledge, this compound, along with two of its dinuclear copper(II) complexes, was first synthesized and characterized in 1992 by researchers from Nankai University (China) [16]. Subsequently, other scientists from the same institution prepared a homodinuclear vanadyl complex containing DMD [17], as well as both homodinuclear (Ln = Gd, Ho, Lu) [18,19] and mononuclear (Ln = La, Ce, Pr, Nd, Sm) [20] lanthanide complexes, with DMD performing as a binucleating or mononucleating ligand, respectively. However, neither the luminescent properties of the complexes or of the DMD ligand itself were explored in these publications. In the present study, we explore the potentiality of the organic ligand DMD as a constituent of the emitting layer for the fabrication of OLEDs. For this purpose, DMD was synthesized and fully characterized, and included herein is the first description of its $^{1}H$ and $^{13}C$ NMR spectra, containing a complete assignment of the signals. Subsequently, several devices were constructed and DMD performance, tested.

## 2. Experimental

### 2.1. Materials

Chemicals were purchased from commercial sources and used without further purification. Reagents employed in the synthesis of the DMD precursor, namely, Hdfmp, and other reagents (isoniazid and the compounds used in the fabrication of the OLED devices) were purchased from Vetec (RJ, Brazil), Fluka (SP, Brazil) and Lumtec Corp. (Taiwan), respectively.

### 2.2. Synthesis and characterization of DMD

2-Hydroxy-5-methylisophthalaldehyde (Hdfmp) was obtained by modifying the method published by Gagné et al. [21]. DMD was prepared based on the reaction between Hdfmp and two equivalents of isoniazid. 10 mL of an ethanolic solution containing isoniazid (0.55 g, 4 mmol) were added dropwise to 20 mL of an ethanolic solution of Hdfmp (0.33 g, 2 mmol). After reflux for 1 h, the system was left to cool until reaching the room temperature and the yellow precipitate formed was filtered off and dried in vacuum. The yellow crystalline powder obtained was dried in open atmosphere. Yield: 80%. m.p. 196 °C (literature: 192–194 °C) [11].

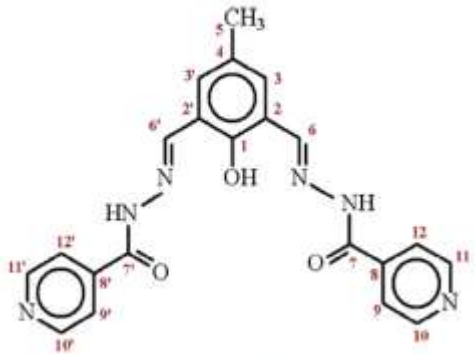

Fig. 1. The chemical structure of DMD with the corresponding atom labeling.

Elemental analysis for $C_{21}H_{18}O_3N_6{\cdot}1\frac{1}{2}\,H_2O$ – Calcd.: C, 58.7%; H, 4.9%; N, 19.6%. Found: C, 58.0%; H, 4.8%; N 19.2%.

**Main IR bands** (KBr): ν(N—H) at 3180; amide I at 1676; amide II at 1553; amide III at 1301 and $\nu(C{=}N)_{azomethine}$ at 1618 $cm^{-1}$.

$^{1}$**H NMR** (DMSO-$d_6$, 400 MHz): δ12.36(s, 2H, **—NH**); δ12.20(s, 1H, **—OH**); δ 8.80 (d, 4H, $^{3}J_{HH}$ = 6.0 Hz, **H10**, **H10'**, **H11**, **H11'**); δ 8.73 (s, 2H, **H6**, **H6'**); δ 7.85 (d, 4H, $^{3}J_{HH}$ = 6.0 Hz, **H9**, **H9'**, **H12**, **H12'**); δ 7.59 (s, 2H, **H3**, **H3'**); δ 2.32 (s, 3H, **—CH$_3$**).

$^{13}$**C NMR** (DMSO-$d_6$, 100 MHz): δ 161.5 (**C7**, **C7'**); δ 154.9 (**C1**); δ 150.4 (**C10**, **C10'**, **C11**, **C11'**); δ 147.3 (**C6**, **C6'**); δ 140.0 (**C8**, **C8'**); δ 130.9 (**C3**, **C3'**); δ 128.5 (**C4**); δ 121.5 (**C9**, **C9'**, **C12**, **C12'**); δ 119.7 (**C2**, **C2'**); δ 19.9 (**C5**).

Since the $^{1}H$ and $^{13}C$ NMR spectra of DMD are described here for the first time, they will be discussed in further detail in Section 3.

### 2.3. Methods

Carbon, nitrogen and hydrogen were determined using a Thermo Electron Corporation CHNS analyzer, model Flash EA 1112. IR spectra were recorded on a Perkin–Elmer FT-IR 2000 spectrometer by the KBr pellet technique. $^{1}H$ and $^{13}C$ NMR DMD spectra were obtained on a Bruker Avance III HD-400 spectrometer (9.4 T, 400 MHz for the $^{1}H$ nuclei) using a 5 mm probe. DMSO-$d_6$ was used as the solvent for these analyses. Calibration of all spectra was performed with the residual solvent peaks as references (2.50 and 39.52 ppm for hydrogen and carbon, respectively) [22]. The chemical shifts (δ) were measured in units of parts per million (ppm). Two-dimensional NMR experiments, namely, $^{1}Hx^{13}C$ HSQC (Heteronuclear Single Quantum Coherence) and HMBC (Heteronuclear Multiple-Bond Correlation) spectroscopies were performed in order to correctly assign the signals in the carbon spectrum.

With the aim of determining the Highest Occupied Molecular Orbital (HOMO) and Lowest Unoccupied Molecular Orbital (LUMO) of DMD, the cyclic voltammetry (CV) technique was employed using a CompactStat potenciostat (Ivium Technologies). Compared with other available techniques, cyclic voltammetry and optical absorption spectroscopy are simple and can be routinely used to control the frontier orbital energies and energy diagrams during the preparation of organic films and devices. In our measurements, the working electrode was composed of graphite, the counter electrode was Pt wire and the reference electrode was Ag/AgCl. The electrolyte was a 0.05 mol $L^{-1}$ $TBAPF_6$ (tetrabutylammonium hexafluorophosphate) solution in dichloromethane. Ferrocene was used as an internal reference to calibrate the system [23–25]. The UV–Vis absorption spectra of different films were recorded on a Hewlett–Packard 8452A diode-array spectrometer. The photoluminescence and electroluminescence spectra were obtained on a Photon Technology International (PTI) fluorescence spectrophotometer.

### 2.4. OLED fabrication

OLEDs were assembled using heterojunctions containing a double and triple-layer structure. Specifically, β-NPB [*N,N*-bis(naphtalen-2-yl)-*N,N*-bis(phenyl)benzidine] was employed as the hole-transporting layer, while DMD alone or as dopant of the emitting layer, as well as BCP (2,9-dimethyl-4,7-diphenyl-1,10-phenanthroline) and the coordination complex $Alq_3$ [tris(8-hydroxyquinolinato)aluminum] were used as the hole blocking and electron transporting layers, respectively. BSBF [2-(9,9-spirobifluoren-2-yl)-9,9-spirobifluorene] was used as the organic matrix to promote the energy transfer from the DMD molecule used as dopant. Finally, a 120 nm thick film of aluminum was deposited as the cathode onto a 0.5 Å thick LiF layer. For the multilayered devices, the emitting layer was prepared by the co-evaporation of DMD and the BSBF host compound from two individual thermal sources.

The nominal concentration of DMD ranged from 25% to 50% in the BSBF matrix and the whole layer thickness was of 35 nm. All the different layers of the devices where sequentially deposited in a high vacuum environment by thermal evaporation onto ITO (indium tin oxide) substrates with a sheet resistance of 15 Ω/square. The ITO substrates were cleaned by ultrasonication using a detergent solution, followed by toluene degreasing and subsequent ultrasonication with pure isopropyl alcohol. Finally, the substrates were dried using nitrogen gas. The base pressure was $6.6 \times 10^{-5}$ Pa, and during the evaporation the pressure was $\sim 10^{-4}$ Pa. The deposition rates for the organic compounds were in the range of 0.3–2 Å/s. The layer thickness was controlled *in situ* through a quartz crystal monitor and confirmed with profilometer measurements. The fabricated devices had an active area of about 2 $mm^2$ and operated in forward bias voltage, with ITO as the positive electrode and Al as the negative one.

The fabricated devices are listed below with the correspondent layer thickness.

| | |
|---|---|
| Device 1 | ITO/β-NPB (25 nm)/DMD(40 nm)/$Alq_3$ (15 nm)/LiF (0.5 nm)/Al (120 nm) |
| Device 2 | ITO/β-NPB (25 nm)/BSBF (35 nm)/BCP (15 nm)/$Alq_3$ (10 nm)/LiF (0.5 nm)/Al (120 nm) |
| Device 3 | ITO/β-NPB (25 nm)/25% DMD in BSBF (35 nm)/BCP (15 nm)/$Alq_3$ (10 nm)/LiF (0.5 nm)/Al (120 nm) |
| Device 4 | ITO/β-NPB (25 nm)/35% DMD in BSBF (35 nm)/BCP (15 nm)/$Alq_3$ (10 nm)/LiF (0.5 nm)/Al (120 nm) |
| Device 5 | ITO/β-NPB (25 nm)/50% DMD in BSBF (35 nm)/BCP (15 nm)/$Alq_3$ (10 nm)/LiF (0.5 nm)/Al (120 nm) |

The electrical and brightness measurements were conducted simultaneously on a LabView based program using a Keithley 2240 and a calibrated Newport Power Meter (model 1830-C) radiometer/photometer. Photoluminescence and electroluminescence spectra were obtained on a Photon Technology International (PTI) fluorescence spectrophotometer. Luminance was measured on a Konica Minolta LS-100 equipment.

## 3. Results and discussion

### 3.1. Synthesis and identity confirmation of DMD

DMD was obtained as a crystalline solid in high yields through a simple protocol involving a condensation reaction between the precursor Hdfmp and two equivalents of the cheap antituberculosis drug isoniazid. The melting point of the compound, its CHN elemental analysis and the IR spectrum in the 4000–450 $cm^{-1}$ range (Appendix, Fig. A.1) confirmed the identity and purity of this dihydrazone.

### 3.2. NMR spectroscopy

The $^1$H spectrum of DMD could be analyzed in a quite straightforward manner. Seven signals are observed throughout the selected spectral window (12.5–1.00 ppm), corresponding to the seven different types of hydrogen in the molecule. In the highly de-shielded region, two singlets at 12.36 and 12.20 ppm, of relative integration 2 and 1, respectively, are related to the —*NH* and the —*OH* nuclei. The choice of an aprotic solvent such as DMSO allowed for the detection of such interchangeable hydrogens. The aromatic region of the spectrum presents four signals: two doublets, each one displaying integration 4, at 8.80 and 7.85 ppm, concerning the two kinds of chemically equivalent pyridine hydrogen atoms, and two singlets, each one displaying integration 2, at 8.73 and 7.59 ppm, assigned, respectively, to the azomethine and the *m*-phenol hydrogens. In both cases, the most de-shielded nuclei are associated to the nuclei that lie close to the electronegative nitrogen atoms. As expected, the singlet associated to the methyl group hydrogens is observed in a quite shielded region, at 2.32 ppm. The signals related to impurities are negligible, constituting an additional proof of pureness.

On the other hand, the $^{13}$C spectrum of DMD displays the expected number of ten signals for a total of twenty-one nuclei, many of them being symmetry-related, as also observed in the $^1$H spectrum. In order to characterize the hydrogenated carbons C3/C3′, C5, C6/C6′, C9/C9′ and C12/C12′, besides C10/C10′ and C11/C11′, a $^1$Hx$^{13}$C HSQC experiment was performed (Appendix, Fig. A.2). The carbon atoms that do not contain hydrogen, with the exception of those of the carbonyl groups, are the most difficult to assign. In this situation, an HMBC experiment, which explores $^1$Hx$^{13}$C couplings through a distance of two and three bonds, was mandatory (Appendix, Fig. A.3).

It is worth noting that, to the best of our knowledge, and as stated in Section 2, this is the first description of the $^1$H and $^{13}$C NMR spectra of DMD. These data are quite important in order to correctly characterize the nature and, to a certain extent, the purity, of the compound whose potentiality as a constituent of the emitting layer for the fabrication of OLEDs was under evaluation.

### 3.3. Absorption spectra

The energy gap ($E_g$) and the ionization potential (IP) of the DMD molecule were estimated from optical and electrochemical techniques [23]. Fig. 2 presents the absorption and emission spectra for a 40 nm thick film of DMD deposited onto a quartz substrate. The absorption shows two bands at 306 nm and 375 nm, with the latter used to determine the optical gap [12]. The excitation of DMD thin films in both absorption peaks always gave a broad band emission in the orange-red region (1931 CIE coordinates, $X = 0.54$; $Y = 0.44$), with maximum at 600 nm and a Stokes shift of 210 nm.

Based on the HOMO energy levels and the energy gap ($E_g$) obtained from cyclic voltammetry measurements and from the absorption spectra, respectively, it was possible to build the rigid diagram of energy levels of the different assembled devices, as in the example shown in Fig. 3.

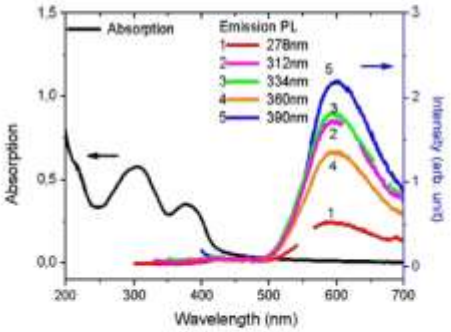


Fig. 2. Absorption and emission spectra of the DMD thin film deposited onto quartz substrate. The broad emission band at 600 nm can be obtained by exciting the DMD molecule in both absorption peaks.

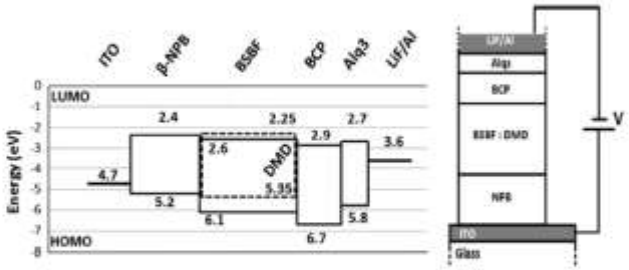


Fig. 3. (Left) Energy diagram of device 3; (Right) DMD HOMO–LUMO levels determined through cyclic voltammetry measurements and absorption spectra. The figure also displays the HOMO–LUMO levels of the other layers with their values obtained from literature.

### 3.4. Devices

Device 1, in which DMD was the only constituent of the emitting layer, did not present any electroluminescence, showing a very high electrical resistance. This can be addressed using the $J$ vs $V$ curve of the Device 1 working in Space Charge Limited Current (SCLC) regime. In this case, we found a charge mobility value of about $(1.4 \pm 0.6) \times 10^{-11}$ cm$^2$/vs. In order to overcome this problem, we used a different approach in which the DMD is used as a dopant in an organic and more conductive matrix (BSBF). For that, it is necessary to use the so called co-deposition technique where the two compounds are thermally deposited at the same time. If there is a good overlap between the dopant (DMD) absorption spectrum and the matrix (BSBF) emission spectrum there is the possibility to promote an energy transfer between them and, consequently, obtain the emission from DMD. BSBF was chosen as the organic matrix due to the partial overlapping existing between the DMD absorption and the BSBF emission bands (Fig. 4a), enabling an energy transfer process [26]. In this case, the mechanism is the Forster energy transfer (FRET) [27], that is a non-radiative process, with a very weak coupling and essentially described by Coulomb dipole–dipole interaction. The efficiency of the FRET is inversely proportional to the sixth power of a distance called Forster radius, $R_F$, that, in our case, was calculated as: $R_F = 2.4$ nm, in good agreement with the typical values reported in literature for similar systems [28].

Devices 3, 4 and 5 were fabricated varying the DMD dopant concentration, at 25%, 35% and 50%, respectively. Fig. 4b details the electroluminescence spectrum of Device 3, where the broad band peaked around 600 nm contains the emissions from the BSBF matrix (373 nm, 393 nm and 414 nm peaks), from $Alq_3$ (520 nm) and from DMD. These contributions are more evident in Fig. 4c, where a deconvolution was performed using $Alq_3$ and DMD emission parameters. The agreement is reasonable, showing that the broad band observed in electroluminescence can be due to both emissions.

The electroluminescence spectra of all the fabricated devices are shown in Fig. 5 as a function of the applied voltage. In all the cases, the DMD emission is not alone and is always superimposed with other bands, demonstrating the difficulty of obtaining an

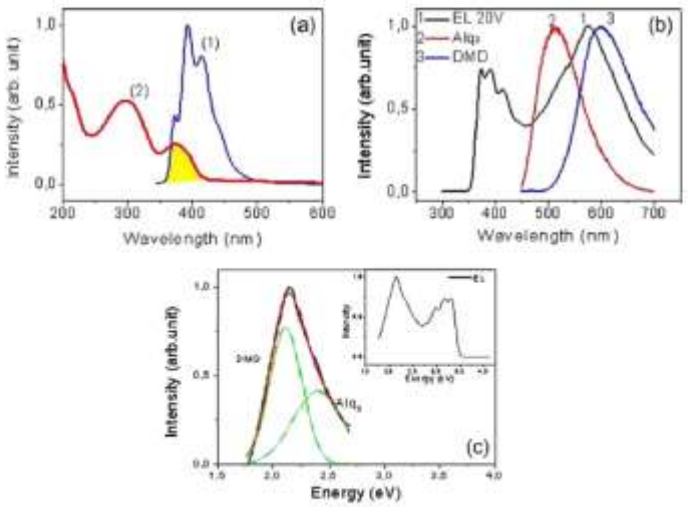


Fig. 4. (a) Overlapping region between DMD absorption (red) and BSBF emission (blue) bands; (b) electroluminescence spectrum of Device 3 (black) alongside the photoluminescence spectra of $Alq_3$ (red) and DMD (blue); (c) deconvolution of the 576 nm band into two contributions: from DMD (2.11 eV) and Alq3 (2.40 eV). (For interpretation of the references to color in this figure legend, the reader is referred to the web version of this article.)

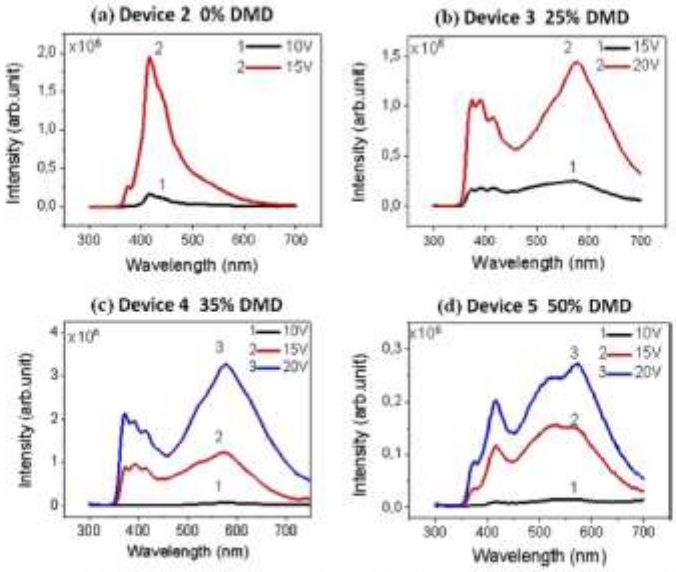


Fig. 5. Electroluminescence spectra of the fabricated devices with different DMD contents: (a) 0% DMD; (b) 25% DMD; (c) 35% DMD; (c) 50% DMD. The other layers were maintained for all the devices. The insets of each figure show a picture of the correspondent device working at 15 V.

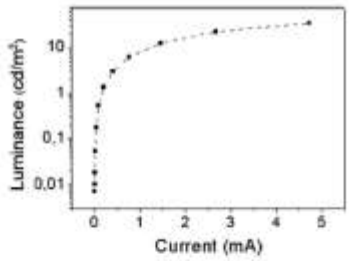


Fig. 6. Device 4 luminance curve as a function of the applied current.

efficient exciton recombination in the DMD layer, probably due to the low efficient energy transfer from the BSBF matrix. In fact, the presence of the matrix emission in the EL spectra is an indication of the charge recombination in this layer. In addition, when increasing the applied voltage, the BCP layer (15 nm) did not demonstrate higher capacity in blocking holes efficiently, thus increasing the $Alq_3$ emission.

An overall analysis of the fabricated devices indicates that the emission intensity from DMD increases as a function of the applied voltage and of its content in the matrix up to 35% (Fig. 5b and c). For 50% of DMD doping, the intensity decreased (Fig. 5d). This behavior can be explained by the low electrical conductivity of DMD, as already observed in Device 1.

Moreover, the EL spectra of Device 2, Fig. 5a, in which the active layer is composed only by the BSBF matrix (without DMD as dopant), shows only an emission at 415 nm from the β-NPB layer and a shoulder at 373 nm from BSBF. These emissions are also present in the electroluminescence of Devices 3, 4 and 5, but the presence of the DMD dopant clearly changes the recombination dynamics of these devices.

Despite the similarity of the EL spectra of Devices 3 and 4, we observed a better performance in the emission intensity of the latter with 35% DMD. This behavior was also verified by luminance measurements as a function of the applied voltage, in a constant current regime. According to Fig. 6, Device 4 achieved a maximum luminance of 34.3 cd/m² at 18 V, corresponding to a luminous efficiency of 0.9% [29].

## 4. Conclusions

A compound derived from the antituberculosis drug isoniazid, namely, *N,N'*-diisonicotinoyl-2-hydroxy-5-methylisophthalalde hyde hydrazone (DMD) was prepared and characterized, including, for the first time, the description of its $^1H$ and $^{13}C$ NMR spectra along with a complete signal assignment. The application of DMD as the emitting layer in the fabrication of organic light emitting diodes was tested. The low electrical conductivity of DMD did not allow for the development of a simple bi- or tri-layer device. In order to overcome this limitation, co-deposited devices were fabricated using the organic molecule BSBF as matrix and DMD as dopant in different nominal concentrations. This configuration allowed for the necessary energy transfer from BSBF and DMD. All the co-deposited fabricated devices presented a broad electroluminescence band, in which it was possible to recognize the DMD emission along with emissions of some of the other organic layers. The best results were obtained with 35% DMD doping, achieving a luminance of about 35 cd/m². Although the developed OLEDs were not optimized, and are obviously far from a practical application, they are interesting and promising due to the application of a new class of molecules based on the isonicotinoyl hydrazone moiety. This class is quite easy to synthesize and enables for a variety of simple chemical modifications. Because of these particularities, it has long since been used in drug development, but its potentialities as a constituent of optical dispositives remain largely unexplored.

**Acknowledgements**

Nicolás A. Rey wishes to thank FAPERJ (Fundação Carlos Chagas Filho de Amparo à Pesquisa do Estado do Rio de Janeiro, Brazil) and CNPq (Conselho Nacional de Desenvolvimento Científico e Tecnológico, Brazil) for the awarded research fellowships. The authors are indebted to Rosana Garrido Gomes for her invaluable help in the NMR analyses, performed at the Central Analytical Facility of the Department of Chemistry (PUC-Rio). R.S.M., R.E.A. and M.C. are grateful for the financial support given by the following agencies: CAPES, CNPq, INEO-INCT, FAPERJ, and PUC-Rio for infrastructure involving the fabrication and characterization of the OLED devices.

**Appendix A. Supplementary material**

Supplementary data associated with this article can be found, in the online version, at http://dx.doi.org/10.1016/j.optmat.2015.12.039.

**References**

[1] R. Narang, B. Narasimhan, S. Sharma, Curr. Med. Chem. 19 (2012) 569–612.
[2] X. Su, I. Aprahamian, Chem. Soc. Rev. 43 (2014) 1963–1981.
[3] E. Gursoy, N.U. Guzeldemirci, Eur. J. Med. Chem. 42 (2007) 320–326.
[4] A. Masunari, L.C. Tavares, Bioorg. Med. Chem. 15 (2007) 4229–4236.
[5] N. Raman, S. Ravichandran, C. Thangaraja, J. Chem. Sci. 116 (2004) 215–219.
[6] B. Szczesna, Z. Urbanczyk-Lipkowska, Supramol. Chem. 13 (2001) 247–251.
[7] A. Bieliauskas, V. Getautis, V. Martynaitis, V. Jankauskas, E. Kamarauskas, S. Kitkitokaityte, A. Šačkus, Synth. Met. 179 (2013) 27–33.
[8] A. Bieliauskas, V. Martynaitis, V. Getautis, T. Malinauskas, V. Jankauskas, E. Kamarauskas, W. Holzer, A. Šačkus, Tetrahedron 68 (2012) 3552–3559.
[9] A.C. González-Baró, R. Pis-Díez, B.S. Parajón-Costa, N.A. Rey, J. Mol. Struct. 1007 (2012) 95–101.
[10] L.V. de Freitas, C.C.P. da Silva, J. Ellena, L.A.S. Costa, N.A. Rey, Spectrochim. Acta Part A – Mol. Biomol. Spectrosc. 116 (2013) 41–48.
[11] R.A. Hauser-Davis, L.V. de Freitas, D.S. Cuiderman, W.S. Cruz, M.C. Mietto, J. Landeira-Fernandez, A.A. Valiente-Gabioud, C.O. Fernandez, N.A. Rey, Metallomics 7 (2015) 743–747.
[12] X.Q. Liu, B.J. Chen, X.H. Zhang, C.S. Lee, H.L. Kwong, S.T. Lee, Chem. Mater. 13 (2001) 456–458.
[13] C. Legnani, S.R. Louro, W.G. Quirino, M. Tabak, M. Cremona, Thin Solid Films 515 (2006) 902–906.
[14] Z.S. Wu, Z.W. An, X.B. Chen, P. Chen, Org. Lett. 15 (2013) 1456–1459.
[15] A.C. Grimsdale, K.L. Chan, R.E. Martin, P.G. Jokisz, A.B. Holmes, Chem. Rev. 109 (2009) 897–1091.
[16] J.T. Chen, D. Liao, R. Zhiang, H. Chen, W. Liu, Chem. J. Chin. Univ. 13 (1992) 6–9.
[17] J.T. Chen, D.Z. Liao, R.H. Zhang, Z.L. Xiong, G.M. Yang, Polyhedron 13 (1994) 1701–1704.
[18] R.H. Zhang, H.M. Wang, D.Z. Liao, J.T. Chen, H.G. Wang, X.K. Yao, Chin. J. Chem. 14 (1996) 506–515.
[19] X.H. Bu, M. Du, L. Zhang, X.B. Song, R.H. Zhang, T. Clifford, Inorg. Chim. Acta 308 (2000) 141–149.
[20] X.H. Bu, Y.X. Gao, W. Chen, H. Liu, R.H. Zhang, J. Rare Earths 19 (2001) 70–73.
[21] R.R. Gagné, C.L. Spiro, T.J. Smith, C.A. Hamann, W.R. Thies, A.K. Shiemke, J. Am. Chem. Soc. 103 (1981) 4073–4081.
[22] H.E. Gottlieb, V. Kotlyar, A. Nudelman, J. Org. Chem. 62 (1997) 7512–7515.
[23] C.M. Cardona, W. Li, A.E. Kaifer, D. Stockdale, G.C. Bazan, Adv. Mater. 23 (2011) 2367–2371.
[24] D.T. Sawyer, A. Sobkowiak, J.L. Roberts, Electrochemistry for Chemists, Wiley, New York, 1995.
[25] T. Förster, Discuss. Faraday Soc. 27 (1959) 7–17.
[26] S.R. Forrest, D.D.C. Bradley, M.E. Thompson, Adv. Mater. 15 (2003) 1043–1048.
[27] T. Förster, 10TH Spies Memorial Lecture Transfer Mechanisms of Electronic Excitation, 1959, pp. 7–17.
[28] B. Valeur, Molecular Fluorescence: Principles and Applications, Wiley-VCH Verlag GmbH, 2001.
[29] C. Adachi, M.A. Baldo, M.E. Thompson, S.R. Forrest, J. Appl. Phys. 90 (2001) 5048–5051.